ELECTRONIC SUPPORTING INFORMATION FOR

The Robust, Readily Available Cobalt(III) Trication $[Co(NH_2CHPhCHPhNH_2)_3]^{3+}$ is a Progenitor of Broadly Applicable Chirality and Prochirality Sensing Agents†

Quang H. Luu,[ꝏ] Kyle G. Lewis,[§] Anik Banerjee,[ꝏ] Nattamai Bhuvanesh, John A. Gladysz*[ꝏ]

Department of Chemistry, Texas A&M University, P.O. Box 30012, College Station, Texas 77842-3012, USA. E-mail: gladysz@mail.chem.tamu.edu

■ **EXPERIMENTAL SECTION (continued)**

General data. NMR spectra were recorded on a Varian NMRS 500 MHz spectrometer at ambient probe temperature. Chemical shifts (δ in ppm) were referenced to residual solvent signals (^{1}H: $CHCl_3$, 7.26; CHD_2CN, 1.94; DMSO-d_5, 2.50; CHD_2OD, 3.30; $CDHCl_2$, 5.32; acetone-d_5, 2.05; ^{13}C: $CDCl_3$, 77.2; DMSO-d_6, 39.5; CD_3OD, 49.0; CD_2Cl_2, 54.0; acetone-d_6, 29.8) or external C_6F_6 (^{19}F, –164.9) or 85 wt% aqueous H_3PO_4 (^{31}P, 0.00). IR spectra were recorded on a Shimadzu IRAffinity-1 spectrometer (Pike MIRacle ATR system, diamond/ZnSe crystal). Melting points were determined using an OptiMelt MPA 100 instrument. Microanalyses were conducted by Atlantic Microlab. HPLC analyses were carried out with a Shimadzu instrument package (pump/autosampler/detector LC-20AD/SIL-20A/SPD-M20A).

NMR solvents (Cambridge Isotopes) were treated as follows: DMSO-d_6, distilled under vacuum and stored over molecular sieves; $CDCl_3$, CD_2Cl_2, acetone-d_6, CD_3CN, and CD_3OD, stored over molecular sieves. HPLC grade solvents (hexanes, Fischer; isopropanol (**38**), JT Baker) were degassed. The following materials were used as received: CH_2Cl_2 (EMD Chemicals, ACS grade), CH_3OH (EMD, anhydrous, 99.8%), acetone (BDH, ACS grade), toluene (BDH, ACS grade), $Co(OAc)_2{\cdot}4H_2O$ (Alfa Aesar, 98%), (*S*,*S*)-dpen ($NH_2CHPhCHPhNH_2$; Oakwood or Combi blocks), activated charcoal (Acros, Norit SX 4), Na^+ BAr_f^- (BAr_f^- = $B(3,5\text{-}C_6H_3(CF_3)_2)_4^-$; Ark Pharm, 97%), aqueous HI (Aldrich, 57 wt%, 99.9%), CoI_2 (Aldrich, anhydrous, 99%), KI (Aldrich, anhydrous, 99%), NaI (EMD, >99.5%), silica gel (Silicycle SiliaFlash® F60), Celite 545 (Aldrich), (*S*)-1-phenethyl amine ((*S*)-**5**, TCI Chemicals, >98%, ee 97+%), 2-carbomethoxy cyclopentanone (**7**, TCI Chemicals, 97%), *D*- and *L*-proline (*R*- and *S*-**9**, Acros Organics, 99%), (*S*)-1-phenylethanol ((*S*)-**10**; Alfa Aesar, 98+%), (*R*)-**10** (Alfa Aesar, 99%, ee 97+%), *DL*-lactide (**11**, Aldrich, 99%), *L*-lactide (*S*,*S*-**11**, Aldrich, 98%), (*S*)- and (*R*)-1,1'-bi-2-naphthol ((*S*)- and (*R*)-BINOL, Ark Pharm, >98%), δ-hexanolactone (**12**, Alfa Aesar, 98%), styrene oxide (**16**, Alfa Aesar, 98%), 1,2-propanediol (**21**, Aldrich, 99%), 1,2-butanediol (**22**, Aldrich, 98%), 2-carbomethoxy cycloheptanone (**23**, Aldrich, 99%), ethyl 2-methylacetoacetate (**24**, Alfa Aesar, 95%), 2-acetylcyclopentanone (**25**, TCI Chemicals, >95%), (*S*)-*tert*-butylsulfinamide

((*S*)-**26**, Ark Pharm, 98%), (*R*)-*tert*-butylsulfinamide ((*R*)-**26**, ACS Scientific, 98%), 2-methyltetrahydofuran (**27**, Aldrich, >99%), 2-bromopropionamide (**30**, Aldrich, 99%), 2-carboethoxy cyclohexanone (**31**, Aldrich, 95%), cyclohexene oxide (**32**, TCI Chemicals, 98%), methyl ethyl ketone (**33**, Aldrich, 99%), chloroacetone (**34**, Acros Organics, 96%), DMSO (**35**, BDH, 99.9%), ethyl acetate (**36**, Aldrich, 99.8%), isopropylamine (**37**, Alfa Aesar, 99%), 1-methyl-2-oxindole (**39**, Aldrich, 97%), ethyl acetoacetate (**40**, Alfa Aesar, 99%), 2-bromoethyl acetate (**41**, TCI Chemicals, >98%), 3-pentanone (**42**, Aldrich, >99%), 2-bromoacetophenone (**43**, Alfa Aesar, 98%), ethyl chloroacetate (**44**, TCI Chemicals, 98%), benzyl carbamate (**45**, Alfa Aesar, 99%), ethyl cyanoacetate (**46**, TCI Chemicals, >98%), propionamide (**47**, TCI Chemicals, >98%), dimethyl malonates (Alfa Aesar, 98%), *sec*-butylbenzene (TCI Chemicals, >99%), nitroethane (Aldrich, >98%), 5-hydroxymethyl-2-pyrrolidinone (Chem-Impex International, 98.5%), propionitrile (Acros Organics, 99%), propionic acid (Alfa Aesar, 99%), methyl isovalerate (Aldrich, >98%), diethyl phosphite (Alfa Aesar, 96%), and tetrahydrofuran (Aldrich, >99%).

The following analytes were synthesized by literature procedures: (*S*)- and (*R*)-1-phenylethyl acetate ((*S*)- and (*R*)-**4**),[s1] 1-phenethyl amine (**5**),[s2] phenyl methyl sulfoxide (**6**),[s3] (*S*)- and (*R*)-Boc-BINOL ((*S*)- and (*R*)-**8**),[s1] (*S*)- and (*R*)-BINOL diacetate,[s1] 1-phenyl-1,2-ethanediol (**14**),[s4] 1-phenyl-2,2,2-trifluoroethanol (**15**),[s5] *N*-tosyl phenethyl amine (**17**),[s6] *N*-acetyl phenethyl amine (**18**),[s2] hydroxyphenylmethyl diethyl phosphonate (**19**),[s7] hydroxyphenylmethyl dimethyl phosphonate (**20**),[s7] 2-phenyl-2-butanol (**28**),[s8] 1-phenyl-1-chloroethane.[s9] and methyl 2-bromopropionate (**29**).[s10] Ibuprofen (**13**) was isolated from commercially available tablets following a literature procedure.[s11]

Alternative syntheses of Λ-[Co((*S*,*S*)-$NH_2CHPhCHPhNH_2)_3]^{3+}$ $3I^-$ (Λ-2^{3+} $3I^-$) directly from cobalt(II) precursors (bypassing Λ-2^{3+} $3Cl^-$ in Scheme 1). **A.** A gas circulating flask[s12] was charged with a solution of CoI_2 (0.156 g, 0.50 mmol) in CH_3OH (50 mL). Activated charcoal (0.05 g) and (*S*,*S*)-dpen (0.356 g, 1.68 mmol, 3.36 equiv) were added with vigorous stirring. Air was passed through the suspension. After 17 h, the mixture was filtered through Celite and aqueous HI (0.377 g, 57 wt%, 1.68 mmol) was added. The solvent was removed by rotary

evaporation to give an orange solid. A portion was dissolved in acetone-d_6. $^{13}C\{^1H\}$ NMR (acetone-d_6, δ in ppm, partial): 62.2 and 64.7 (2s, ca. 2:1, **C**HPh, Λ and Δ-**2**$^{3+}$ 3I$^-$).[s13] The solid was dissolved in 95:5 v/v CH_2Cl_2/CH_3OH (1 mL). The solution was loaded on a silica gel column (2 × 15 cm) packed in CH_2Cl_2, which was eluted with CH_2Cl_2/CH_3OH (100:0 v/v, 200 mL; 98:2 v/v, 500 mL; 97:3 v/v as needed). The orange band was collected. Solvents were removed by rotary evaporation. The residue was dried by oil pump vacuum at room temperature (20 h) to give Λ-**2**$^{3+}$ 3I$^-$·H_2O (0.208 g, 0.190 mmol, 38%) as an orange solid. **B**. A solution of $Co(OAc)_2$ ·4H_2O (0.296 g, 1.19 mmol) in CH_3OH (50 mL), activated charcoal (0.1 g), (*S*,*S*)-dpen (0.849 g, 4.00 mmol, 3.36 equiv), air, Celite, and aqueous HI (0.898 g, 57 wt%, 4.00 mmol) were combined in a procedure analogous to that in A. A similar workup (3 mL 95:5 v/v CH_2Cl_2/CH_3OH) gave Λ-**2**$^{3+}$ 3I$^-$·H_2O (0.611 g, 0.559 mmol, 47%) as an orange solid, mp 200-201 °C dec (open capillary). Anal. Calcd. for $C_{42}H_{48}CoI_3N_6$·H_2O (1094.05): C 46.09, H 4.60, N 7.68; found C 46.16, H 4.75, N 7.46.

NMR (acetone-d_6, δ in ppm): ^1H (500 MHz) 7.57-7.54 (m, 12H, *o*-Ph), 7.53 (br s, 6H, N**H**H', partial overlap with *o*-Ph), 7.32-7.22 (m, 18H, *m*-, *p*-Ph), 5.63 (br s, 6H, NH**H'**), 5.25 (s, 6H, C**H**Ph), 2.83 (br s, 7H, $\mathbf{H_2}$O); $^{13}C\{^1H\}$ (125 MHz) 130.3 (s, *i*-Ph), 130.0 (s, *p*-Ph), 129.6 and 128.8 (2 s, *o*- and *m*-Ph), 63.2 (s, **C**HPh).

Extended Bibliography. Additional literature that augments that given in the main text is supplied at the end of the references (other CSAs from 2014-present,[s14-s29] other NMR methods for prochirality sensing[s30-s35]).

Table s1. Expansion of Table 1 showing the separation of all aliphatic ^{1}H NMR signals (Δδ, ppm) of the enantiomers of racemic 1-phenylethyl acetate (**4**).

Entry	CSA	Solvent	Δδ (ppm) PhC***H***(CH_3)O	Δδ (ppm) O(C=O)C***H***$_3$	Δδ (ppm) PhCH(C***H***$_3$)O
1	Λ-**1**$^{3+}$ 3BAr$_f^-$	CD_2Cl_2	—	—	—
2	Λ-**2**$^{3+}$ 2Cl$^-$BAr$_f^-$	CD_2Cl_2	1.32	0.50	0.28
3	Δ-**2**$^{3+}$ 2Cl$^-$BAr$_f^-$	CD_2Cl_2	0.15	0.02	—
4	Λ-**2**$^{3+}$ 2Cl$^-$$(C_6F_5)_4^-$	CD_2Cl_2	1.37	0.53	0.28
5	Λ-**2**$^{3+}$ 3BAr$_f^-$	CD_2Cl_2	0.34	0.15	0.08
6	Λ-**2**$^{3+}$ 2I$^-$BAr$_f^-$	CD_2Cl_2	1.30	0.52	0.25
7	Λ-**2**$^{3+}$ 2I$^-$BAr$_f^-$	$CDCl_3$	1.75	0.68	0.37
8	Λ-**2**$^{3+}$ 2I$^-$BAr$_f^-$	acetone-d$_6$	—	—	—
9	Λ-**2**$^{3+}$ 2I$^-$BAr$_f^-$	CD_3CN	—	—	—
10	Λ-**2**$^{3+}$ 2I$^-$BAr$_f^-$	DMSO-d$_6$	—	—	—
11	Λ-**2**$^{3+}$ 2Cl$^-$BAr$_f^-$	acetone-d$_6$	—	—	—
12	Λ-**2**$^{3+}$ 2Cl$^-$BAr$_f^-$	CD_3CN	—	—	—
13	Λ-**2**$^{3+}$ 2Cl$^-$BAr$_f^-$	DMSO-d$_6$	—	—	—

Comparison of ee values obtained by NMR and HPLC (Figure s1). Standard solutions of (*R*)- and (*S*)-**4** were prepared in hexanes/isopropanol (99:1 v/v, 0.0010 g/mL). These were mixed at different ratios into five separate volumetric flasks so that the total volume was always 1.00 mL (Table s2). Each was assayed by HPLC (Chiralcel OD-H column, hexane/isopropanol 99:1 v/v, 0.5 mL/min, 254 nm). The HPLC samples were concentrated by rotary evaporation, redissolved in CD_2Cl_2 (0.70 mL), and transferred to 5 mm NMR tubes. Then Λ-$\mathbf{2}^{3+}$ $2Cl^-$ $BAr_f^-\cdot 2H_2O$ (0.0085 g, 0.0050 mmol) was added and ^{1}H NMR spectra were recorded. Data: Table s2.

Table s2. Tabular comparison of ee values of scalemic **4** obtained by NMR and HPLC.

sample	(*R*)-**4** (mL)[a]	(*S*)-**4** (mL)[a]	theoretical ee (%)	HPLC ee (%)[b]	NMR ee (%)[b]
1	0.940	0.060	+88	+88	+88
2	0.800	0.200	+60	+60	+60
3	0.660	0.340	+32	+32	+32
4	0.220	0.780	–56	–56	–56
5	0.050	0.950	–90	–90	–90

[a]Per the experimental procedure, the volumes represent the ratios of the enantiomers in the samples assayed. [b]The original traces and spectra are depicted in Figures s2-s6.

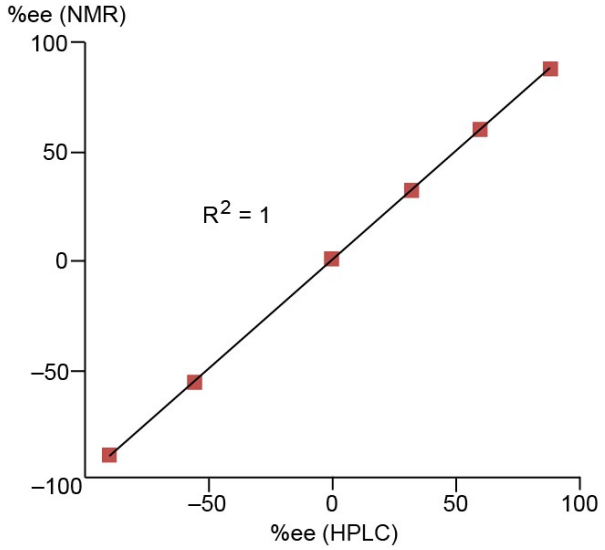

Figure s1. Graphical comparison of ee values of scalemic **4** obtained by NMR and HPLC.

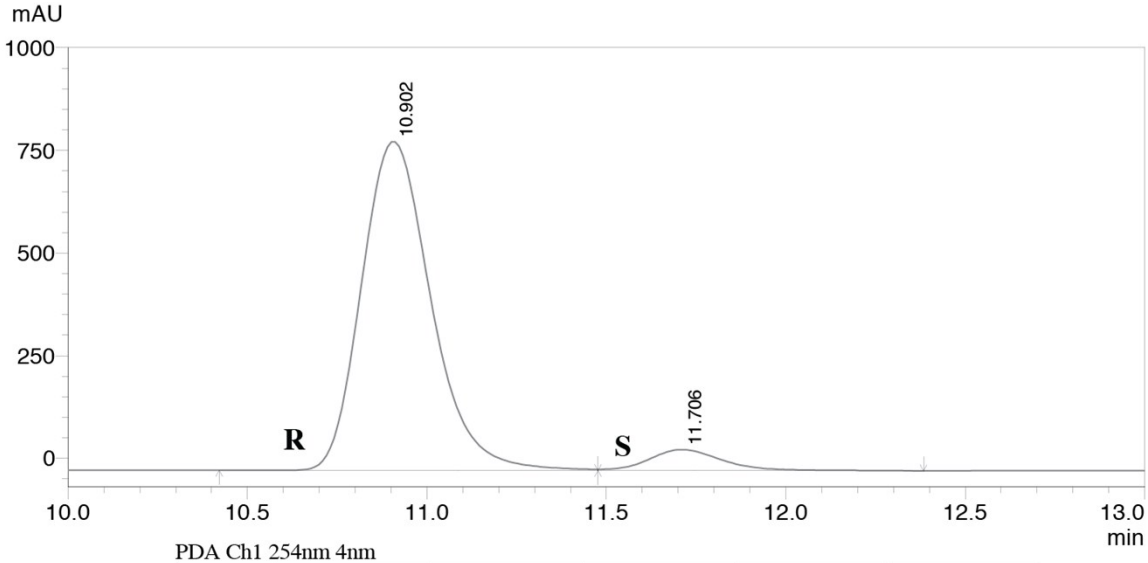

PDA Ch1 254nm 4nm

Peak#	Ret. Time	Area	Height	Area %	Height %
1	10.902	10801926	800685	93.679	93.979
2	11.706	728913	51298	6.321	6.021
Total		11530838	851984	100.000	100.000

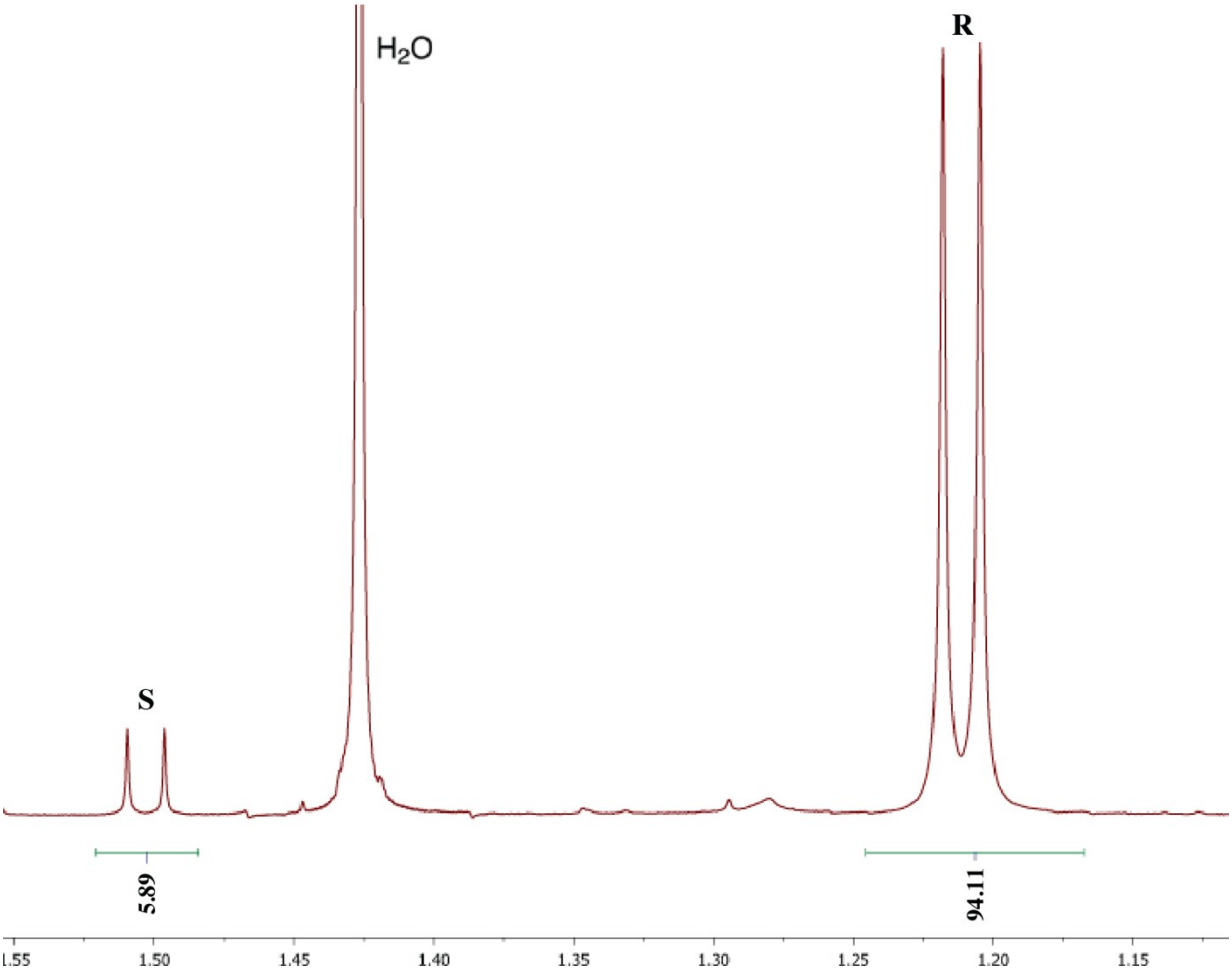

Figure s2. HPLC trace (top) and ^{1}H NMR spectrum (bottom) of **4** (88% ee) corresponding to the data in Table s2.

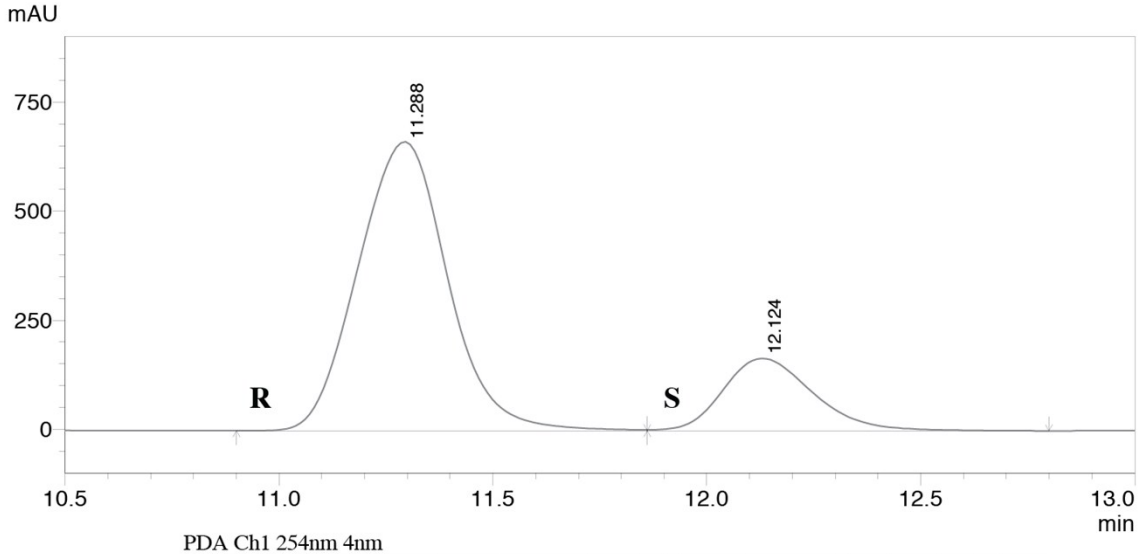

PDA Ch1 254nm 4nm

Peak#	Ret. Time	Area	Height	Area %	Height %
1	11.288	9643154	661589	79.945	79.961
2	12.124	2419045	165801	20.055	20.039
Total		12062199	827390	100.000	100.000

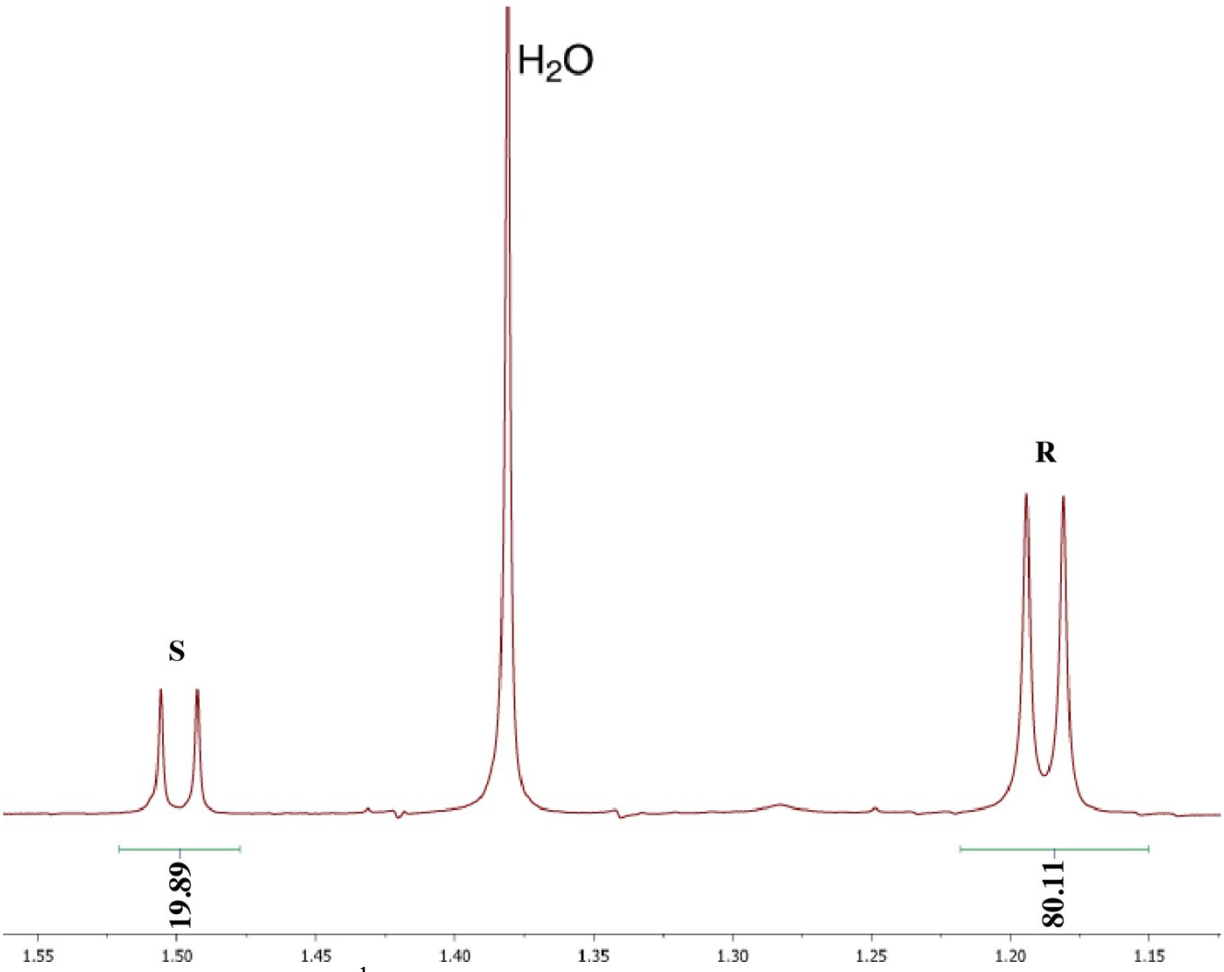

Figure s3. HPLC trace (top) and ^{1}H NMR spectrum (bottom) of **4** (60% ee) corresponding to the data in Table s2.

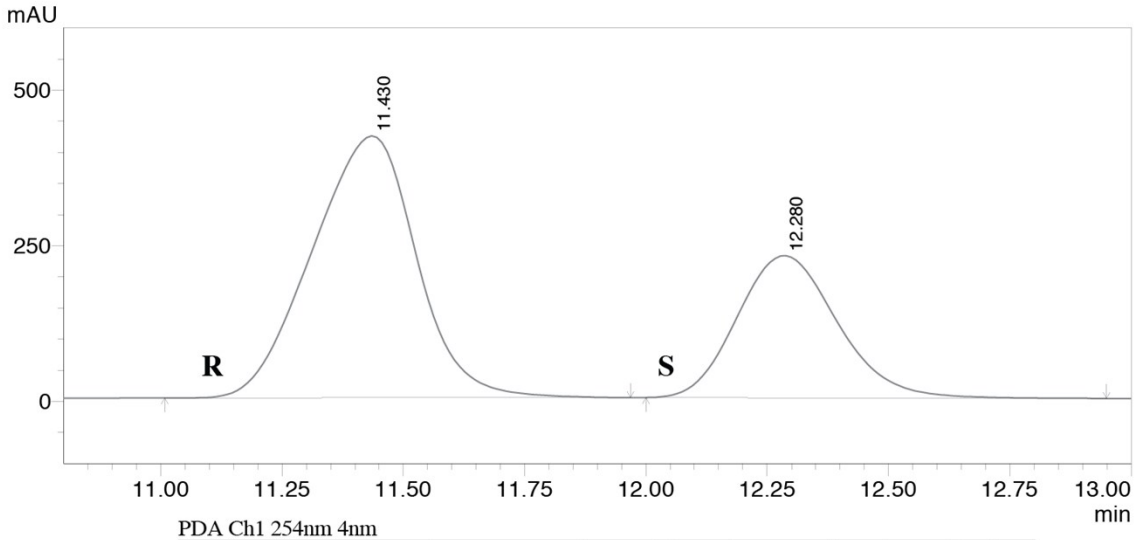

PDA Ch1 254nm 4nm

Peak#	Ret. Time	Area	Height	Area %	Height %
1	11.430	6300989	420643	65.750	64.822
2	12.280	3282337	228272	34.250	35.178
Total		9583326	648915	100.000	100.000

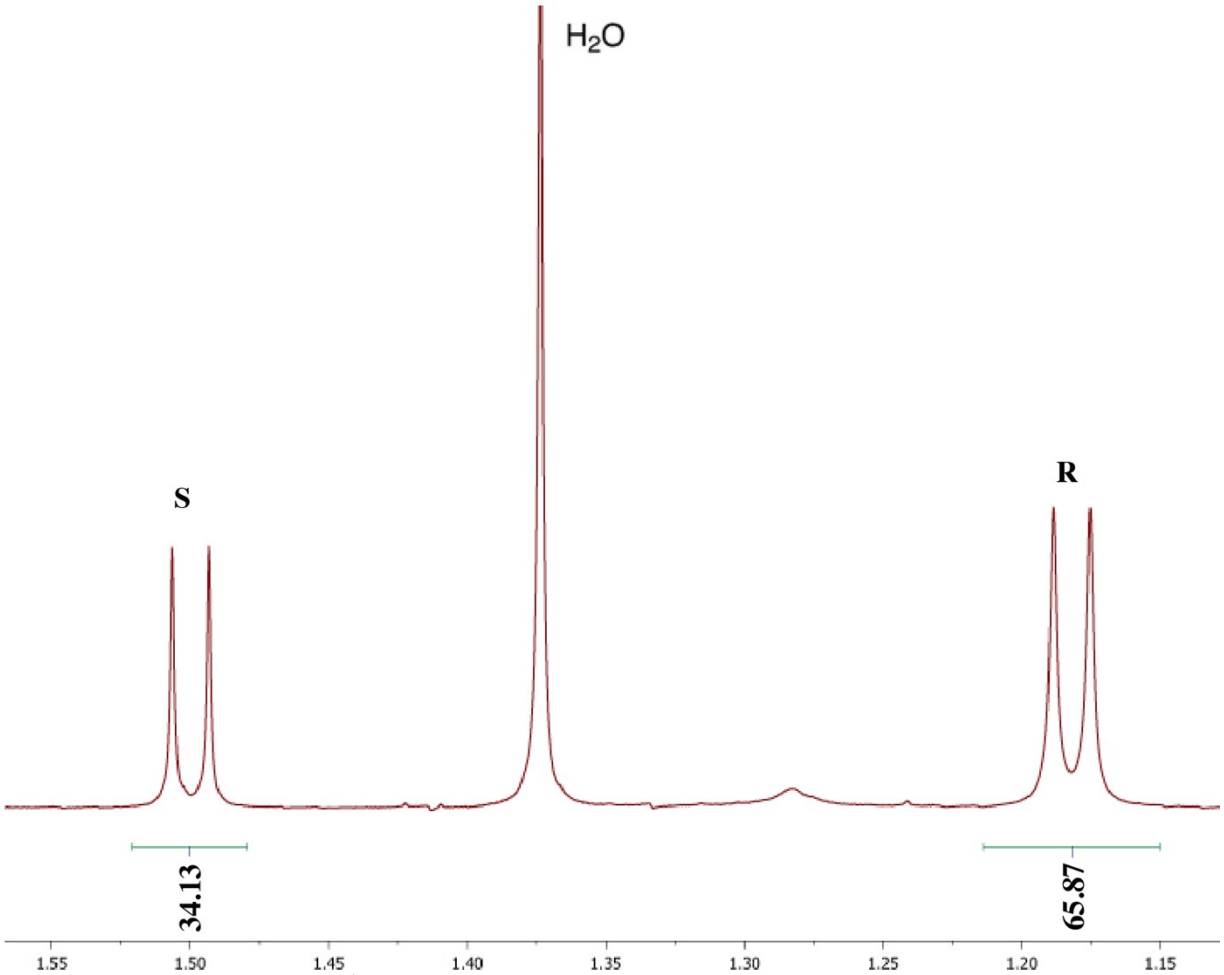

Figure s4. HPLC trace (top) and ^{1}H NMR spectrum (bottom) of **4** (32% ee) corresponding to the data in Table s2.

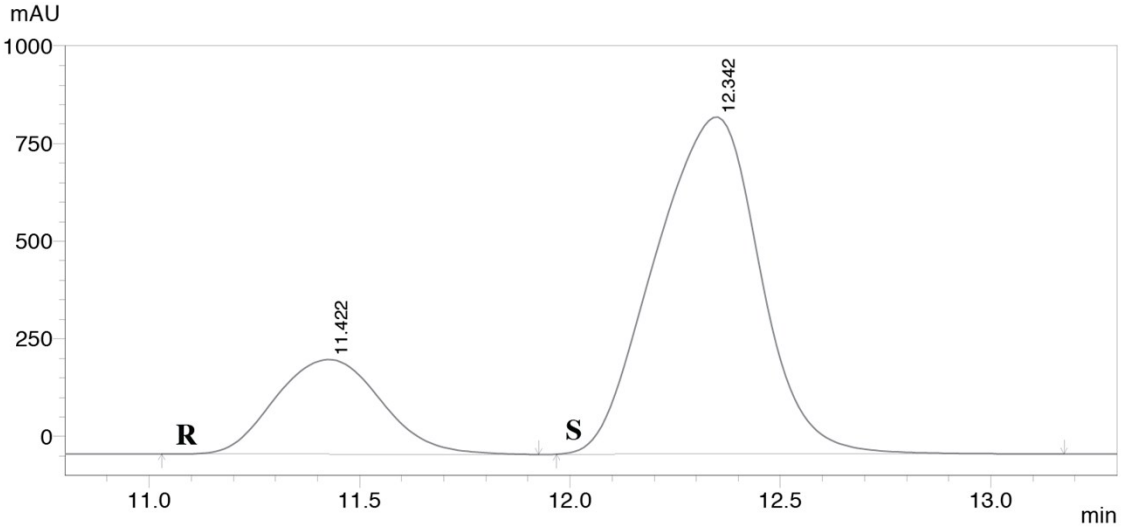

PDA Ch1 254nm 4nm

Peak#	Ret. Time	Area	Height	Area %	Height %
1	11.422	4252585	242308	22.088	21.927
2	12.342	14999902	862736	77.912	78.073
Total		19252487	1105045	100.000	100.000

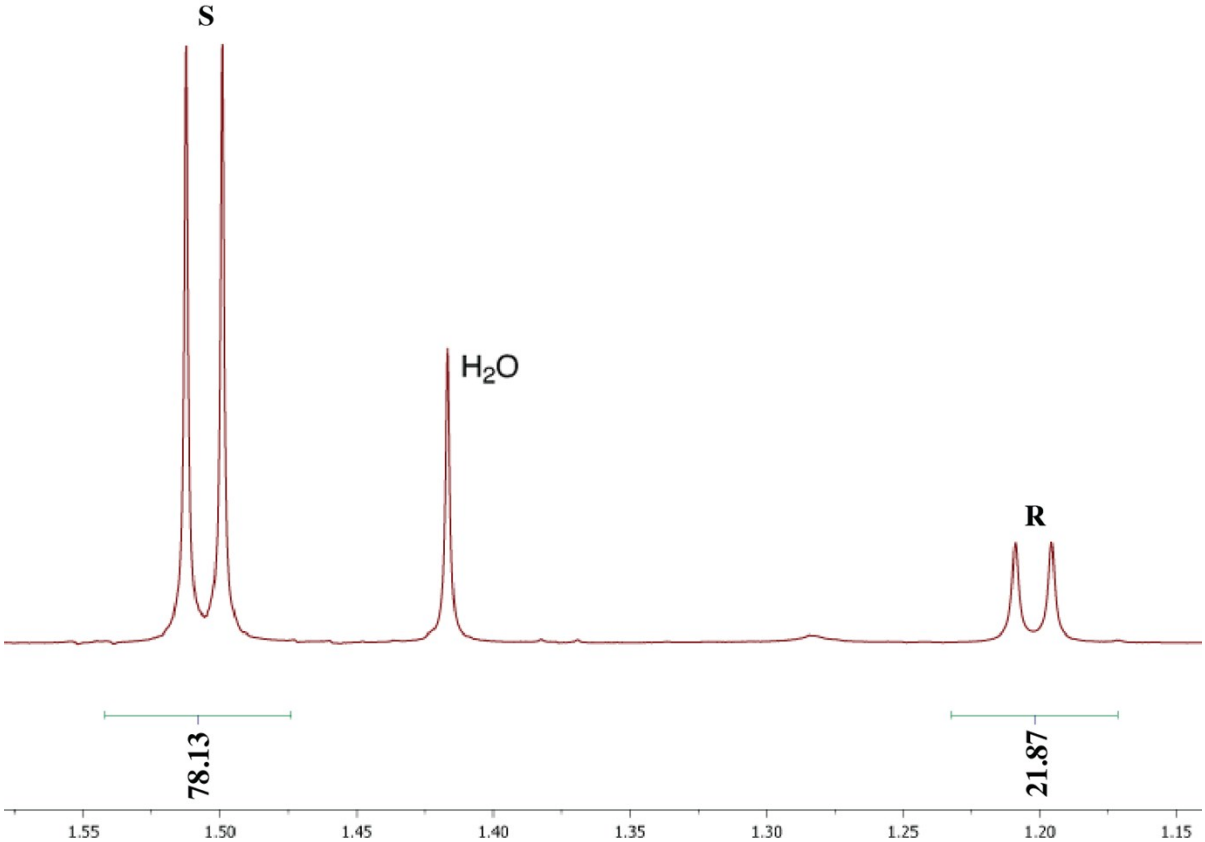

Figure s5. HPLC trace (top) and ^{1}H NMR spectrum (bottom) of **4** (–56% ee) corresponding to the data in Table s2.

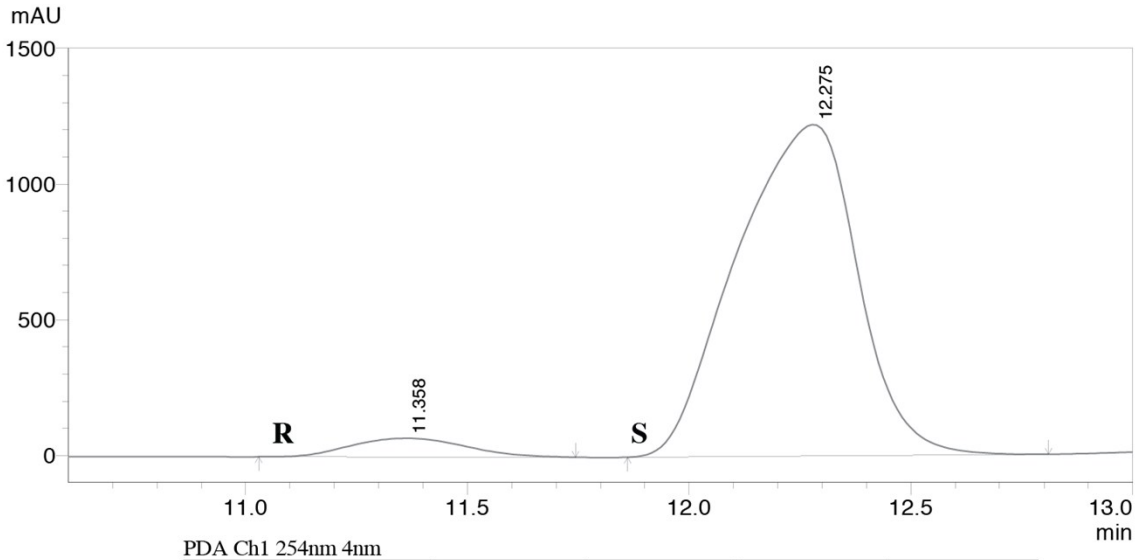

PDA Ch1 254nm 4nm

Peak#	Ret. Time	Area	Height	Area %	Height %
1	11.358	1239908	68869	5.066	5.336
2	12.275	23235959	1221729	94.934	94.664
Total		24475867	1290599	100.000	100.000

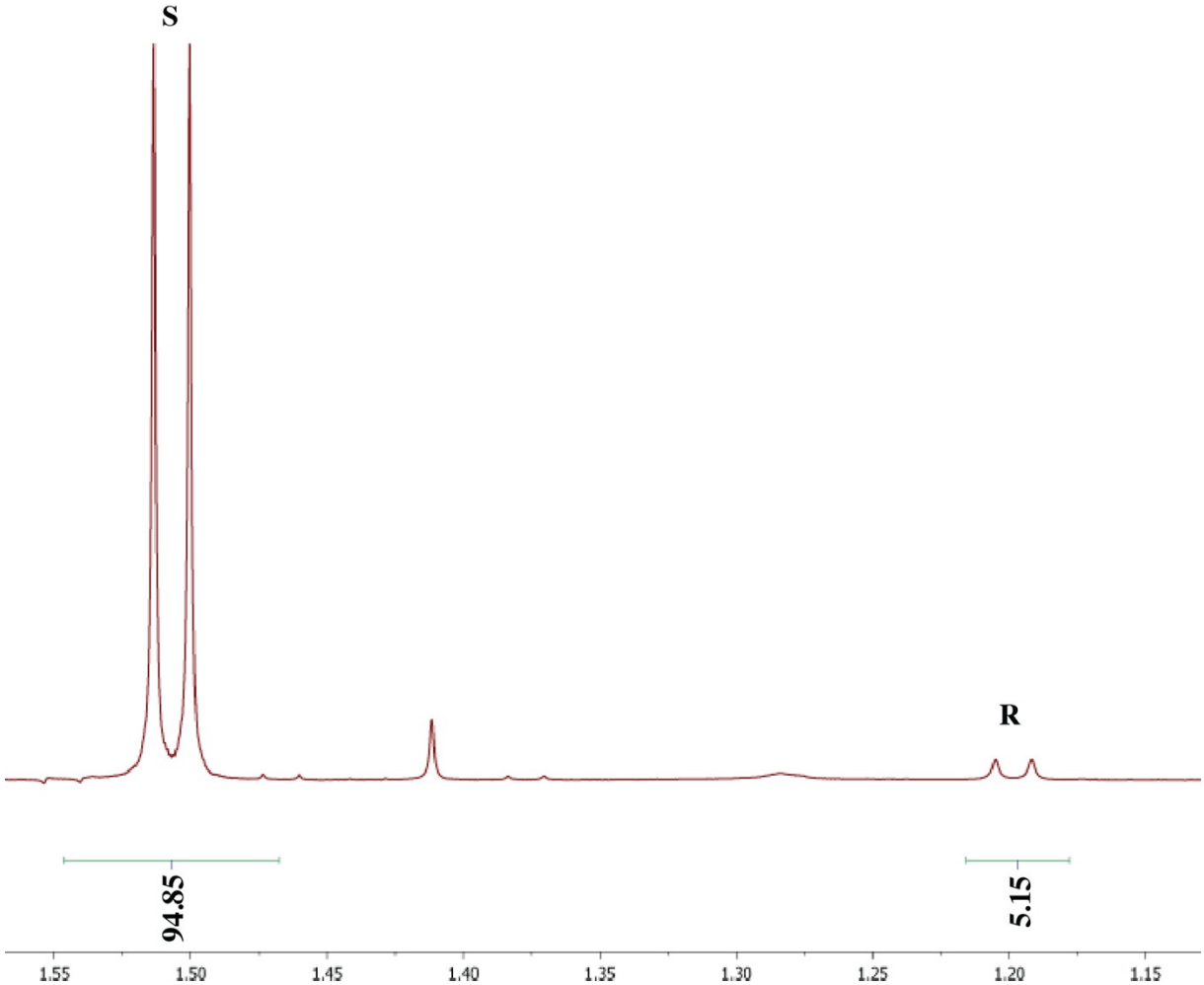

Figure s6. HPLC trace (top) and ^{1}H NMR spectrum (bottom) of **4** (–90% ee) corresponding to the data in Table s2.

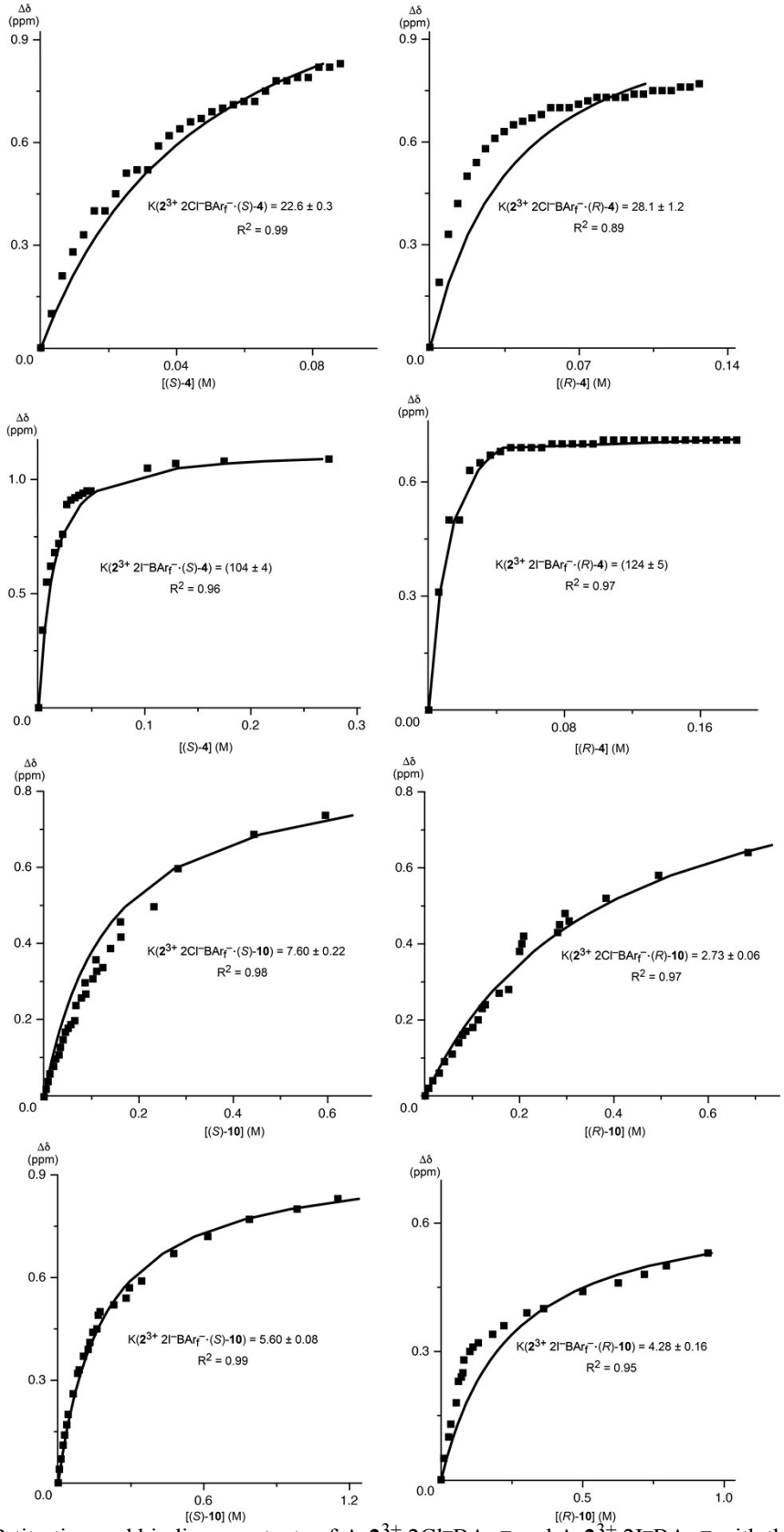

Figure s7. NMR titration and binding constants of Λ-**2**$^{3+}$ 2Cl^{-}BAr$_f^{-}$ and Λ-**2**$^{3+}$ 2I^{-}BAr$_f^{-}$ with the analytes (*S*)-**4**, (*R*)-**4**, (*S*)-**10**, and (*R*)-**10**; raw data underlying Table 4.

Table s3. Summary of crystallographic data for Λ-**2**$^{3+}$ 3I^{-}·6DMSO.[a]

empirical formula	$C_{108}H_{168}Co_2I_6N_{12}O_{12}S_{12}$[a]
formula weight	3080.44
temperature of collection [K]	110.0
diffractometer	Bruker Quest
wavelength [Å]	0.71073
crystal system	monoclinic
space group	*P*2(1)
unit cell dimensions:	
a [Å]	23.057(2)
b [Å]	13.6098(12)
c [Å]	23.378(2)
α [deg]	90
β [deg]	110.977(2)
γ [deg]	90
V [Å^3]	6849.8(10)
Z	2[a]
ρ_{calc} [Mg/m^3]	1.494
absorption coefficient [mm^{-1}]	1.832
F(000)	3100
Crystal size [mm^3]	0.257 × 0.098 × 0.081
Θ [deg]	2.314 to 24.763
range / indices (*h*, *k*, *l*)	–27,26; –16,15; –27,27
reflections collected	72270
independent reflections	22606 [R(int) = 0.0476]
completeness to Θ = 24.763°	98.8%
absorption correction	semiempirical from equivalents
max. and min. transmission	0.4283 and 0.3391
refinement method	full-matrix least-squares on F^2
data / restraints / parameters	22606 / 2887 / 1441
goodness-of-fit on F^2	1.214
final R indices [I>2σ(I)]	*R*1 = 0.0820, w*R*2 = 0.1405
R indices (all data)	*R*1 = 0.0993, w*R*2 = 0.1521
absolute structure parameter	0.08(3)
largest diff. peak and hole [e.Å^{-3}]	4.180 / –1.492

[a]There are two independent molecules in the unit cell. Hence, there are two cobalt atoms in the empirical formula and the *Z* value represents the total number of dicobalt units.

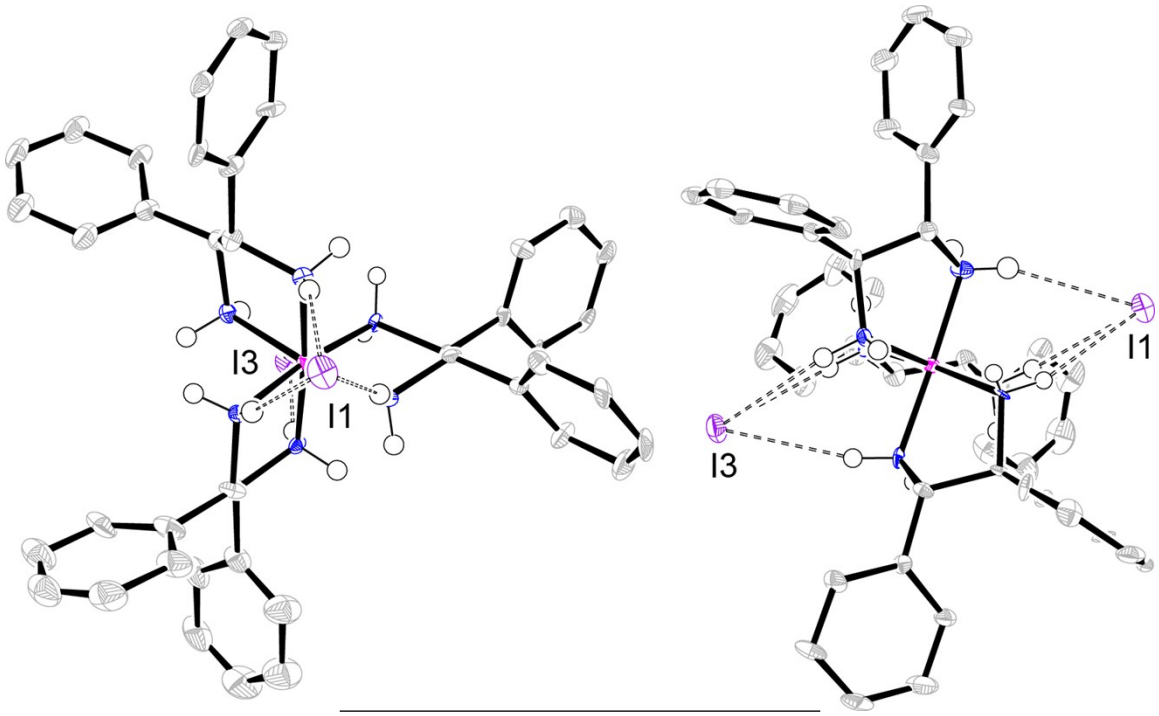

iodide	I···HN (C_3)	I···N	I···H-N
I1	2.826 2.799[a]	3.712 3.675	164.7 166.6
I1	2.794 2.820[a]	3.681 3.700	165.2 163.0
I1	2.771 2.693[a]	3.664 3.585	167.3 166.6
I3	2.835 2.783[a]	3.687 3.652	156.4 160.5
I3	2.725 2.609[a]	3.612 3.506	165.5 168.6
I3	2.760 2.798[a]	3.633 3.672	161.3 161.5

[a]The second set of values is for the other independent molecule in the unit cell, which is geometrically similar.

Figure s8. Thermal ellipsoid diagrams (50% probability level) showing interactions of two iodide anions with the trication of Λ-**2**$^{3+}$ 3I$^-$·6DMSO (*lel*$_3$) viewed along the idealized C_3 axis (left) and one idealized C_2 axis (right). The other independent molecule is similar.

Table s4. Distances (Å) between hydrogen bonded DMSO and NH units depicted in Figure 7.

O atom	O···HN (C_2)	O···N	O···H-N
O1	2.026	2.893	159.1
	2.039[a]	2.882	153.6
O2	2.265	2.923	147.6
	2.141[a]	2.965	150.2
O3	2.290	3.006	135.5
	2.256[a]	3.011	140.1
O4	1.975	2.869	167.0
	2.013[a]	2.859	154.1
O5	2.085	2.870	143.9
	2.074[a]	2.897	149.8
O6	2.197	2.999	146.7
	2.219[a]	2.969	139.2

[a]The second set of values is for the other independent molecule in the unit cell, which is geometrically similar.

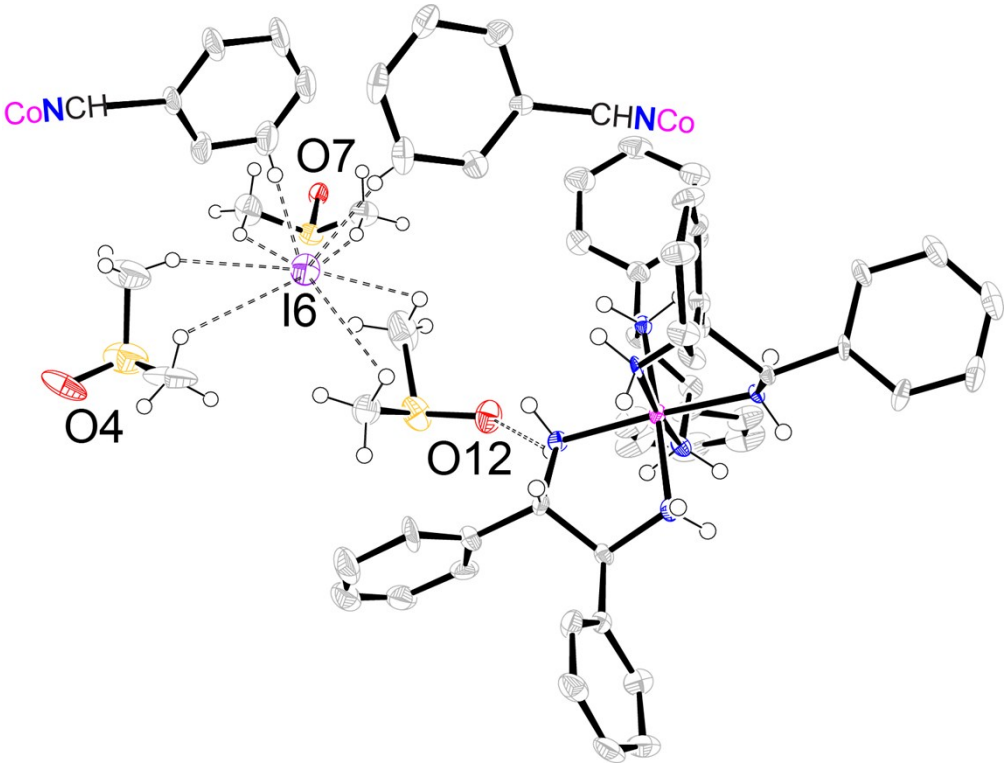

I···HC (3 DMSO)	I···C (3 DMSO)
4.043, 3.081, 3.083, 3.100, 3.321, 3.947	3.910, 3.938, 3.946, 3.992, 4.113, 4.294
I···HC (2 Ph)	I···C (2 Ph)
3.027, 3.285	3.921, 4.057

Figure s9. Thermal ellipsoid diagram (50% probability level) showing the nearest contacts of the third iodide anion in Λ-**2**$^{3+}$ 3I^{-}·6DMSO (molecule 1) with neighboring atoms (CH of three DMSO molecules and two phenyl rings).

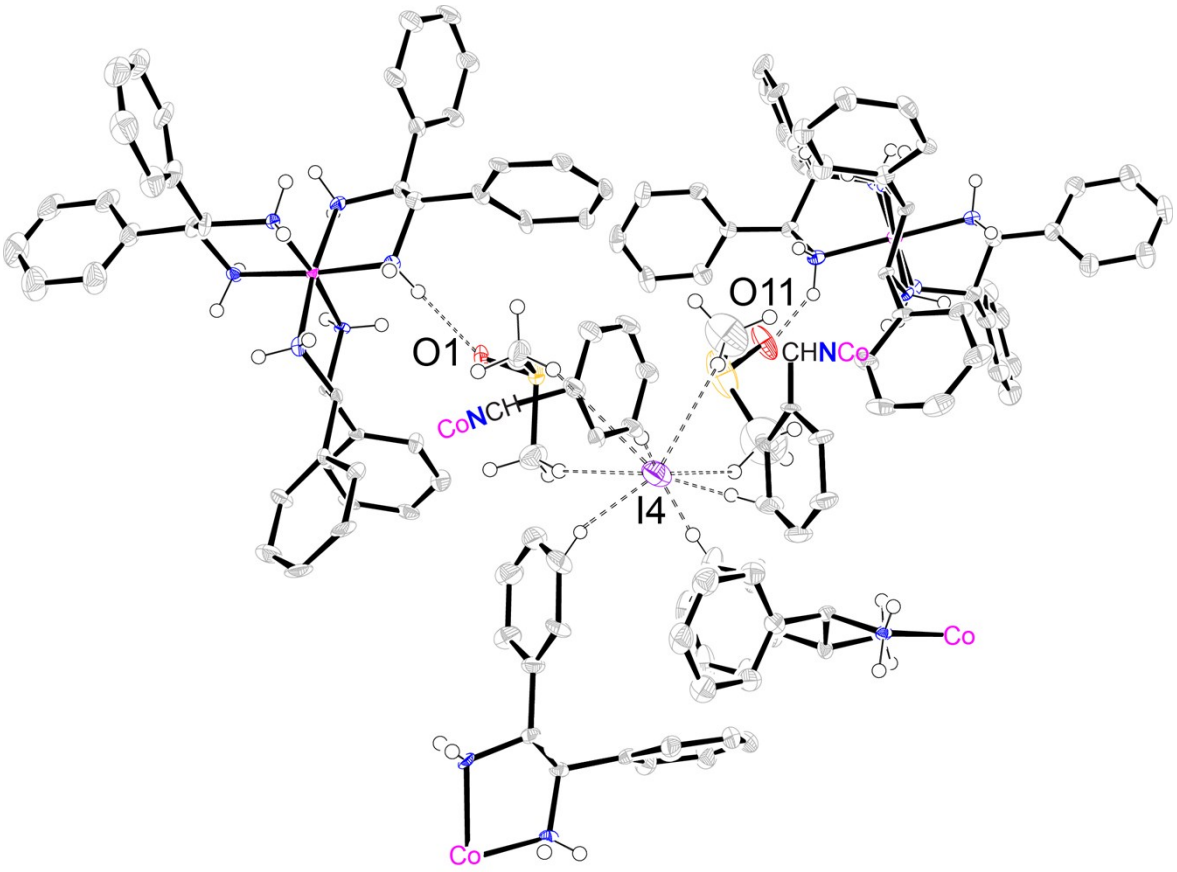

I···HC (2 DMSO)	I···C (2 DMSO)
2.996, 3.116, 3.120, 3.494	3.941, 4.028, 4.069, 4.165
I···HC (4 Ph)	I···C (4 Ph)
3.060, 3.082, 3.123, 3.151	3.848, 3.876, 4.039, 4.068

Figure s10. Thermal ellipsoid diagram (50% probability level) showing the nearest contacts of the third iodide anion in Λ-**2**$^{3+}$ 3I^{-}·6DMSO (molecule 2) with neighboring atoms (CH of two DMSO molecules and four phenyl rings).

Table s5. Key interatomic distances (Å) and angles (°) in crystalline Λ-$\mathbf{2}^{3+}$ $3I^{-}\cdot 6DMSO$.

molecule 1[a]		molecule 2[a]	
Co(1)-N(1B)	1.973(13)	Co(1D)-N(1D)	1.958(12)
Co(1)-N(2B)	1.986(13)	Co(1D)-N(2D)	1.996(13)
Co(1)-N(3B)	1.951(12)	Co(1D)-N(3D)	1.977(12)
Co(1)-N(4B)	1.944(12)	Co(1D)-N(4D)	1.963(12)
Co(1)-N(5B)	1.949(12)	Co(1D)-N(5D)	1.952(13)
Co(1)-N(6B)	1.971(12)	Co(1D)-N(6D)	1.977(12)
N(1B)-C(1B)	1.516(19)	N(1D)-C(1D)	1.504(19)
N(2B)-C(8B)	1.49(2)	N(2D)-C(8D)	1.494(19)
N(3B)-C(6)	1.509(19)	N(3D)-C(15D)	1.490(18)
N(4B)-C(13)	1.49(2)	N(4D)-C(22D)	1.49(2)
N(5B)-C(1I)	1.484(19)	N(5D)-C(36D)	1.487(19)
N(6B)-C(1A)	1.493(18)	N(6D)-C(29D)	1.501(18)
I(2)···HN(2B)	2.783	I(1)···HN(1D)	2.826
I(2)···HN(4B)	2.609	I(1)···HN(3D)	2.794
I(2)···HN(6B)	2.798	I(1)···HN(5D)	2.771
I(5)···HN(1B)	2.799	I(3)···HN(2D)	2.835
I(5)···HN(3B)	2.820	I(3)···HN(4D)	2.725
I(5)···HN(5B)	2.693	I(3)···HN(6D)	2.760
I(6)···HC(2C)	4.059	I(4)···HC(1P)	3.120
I(6)···HC(1AA)	3.081	I(4)···HC(1Q)	2.996
I(2)···N(2B)	3.652	I(1)···N(1D)	3.712
I(2)···N(4B)	3.506	I(1)···N(3D)	3.681
I(2)···N(6B)	3.672	I(1)···N(5D)	3.664
I(5)···N(1B)	3.675	I(3)···N(2D)	3.687
I(5)···N(3B)	3.700	I(3)···N(4D)	3.612
I(5)···N(5B)	3.585	I(3)···N(6D)	3.633
I(6)···C(2C)	4.294	I(4)···C(1P)	4.028
I(6)···C(1AA)	3.938	I(4)···C(1Q)	3.941
O(7)···HN(3B)	2.074	O(1)···HN(1D)	2.062
O(8)···HN(2B)	2.219	O(2)···HN(6D)	2.265
O(9)···HN(4B)	2.256	O(3)···HN(4D)	2.290
O(10)···HN(6B)	2.141	O(4)···HN(5D)	1.975
O(11)···HN(1B)	2.039	O(5)···HN(3D)	2.085
O(12)···HN(5B)	2.013	O(6)···HN(2D)	2.197
O(7)···N(3B)	2.897	O(1)···N(1D)	2.893

O(8)···N(2B)	2.969	O(2)···N(6D)	2.923
O(9)···N(4B)	3.011	O(3)···N(4D)	3.006
O(10)···N(6B)	2.965	O(4)···N(5D)	2.869
O(11)···N(1B)	2.882	O(5)···N(3D)	2.870
O(12)···N(5B)	2.859	O(6)···N(2D)	2.999
N(1B)-Co(1)-N(2B)	85.0(5)	N(1D)-Co(1D)-N(2D)	84.7(5)
N(3B)-Co(1)-N(1B)	92.8(5)	N(1D)-Co(1D)-N(3D)	91.1(5)
N(3B)-Co(1)-N(2B)	92.6(5)	N(1D)-Co(1D)-N(4D)	174.6(5)
N(3B)-Co(1)-N(6B)	172.5(5)	N(1D)-Co(1D)-N(6D)	94.2(5)
N(4B)-Co(1)-N(1B)	176.4(5)	N(3D)-Co(1D)-N(2D)	93.3(5)
N(4B)-Co(1)-N(2B)	92.8(5)	N(4D)-Co(1D)-N(2D)	92.8(5)
N(4B)-Co(1)-N(3B)	84.4(5)	N(4D)-Co(1D)-N(3D)	84.1(5)
N(4B)-Co(1)-N(5B)	93.1(5)	N(4D)-Co(1D)-N(6D)	90.7(5)
N(4B)-Co(1)-N(6B)	89.0(5)	N(5D)-Co(1D)-N(1D)	88.7(5)
N(5B)-Co(1)-N(1B)	89.3(5)	N(5D)-Co(1D)-N(2D)	172.2(5)
N(5B)-Co(1)-N(2B)	173.3(5)	N(5D)-Co(1D)-N(3D)	91.0(5)
N(5B)-Co(1)-N(3B)	91.4(5)	N(5D)-Co(1D)-N(4D)	94.0(5)
N(5B)-Co(1)-N(6B)	85.4(5)	N(5D)-Co(1D)-N(6D)	84.5(5)
N(6B)-Co(1)-N(1B)	93.9(5)	N(6D)-Co(1D)-N(2D)	91.8(5)
N(6B)-Co(1)-N(2B)	91.3(5)	N(6D)-Co(1D)-N(3D)	172.9(5)
I(2)···H(2BA)-N(2B)	160.5	I(1)···H(1DA)-N(1D)	164.7
I(2)···H(4BA)-N(4B)	168.6	I(1)···H(3DA)-N(3D)	165.2
I(2)···H(6BA)-N(6B)	161.5	I(1)···H(5DA)-N(5D)	167.3
I(5)···H(1BA)-N(1B)	161.7	I(3)···H(2DA)-N(2D)	156.4
I(5)···H(3BA)-N(3B)	163.0	I(3)···H(4DA)-N(4D)	165.5
I(5)···H(5BA)-N(5B)	166.6	I(3)···H(6DA)-N(6D)	161.3
I(6)···H(2CA)-C(2C)	97.2	I(4)···H(1PB)-C(1P)	154.7
I(6)···H(1AB)-C(1AA)	146.5	I(4)···H(1QB)-C(1Q)	162.6
O(7)···H(3BB)-N(3B)	149.8	O(1)···H(1DB)-N(1D)	159.1
O(8)···H(2BB)-N(2B)	139.2	O(2)···H(6DB)-N(6D)	147.6
O(9)···H(4BB)-N(4B)	140.1	O(3)···H(4DB)-N(4D)	135.5
O(10)···H(6BB)-N(6B)	150.2	O(4)···H(5DB)-N(5D)	167.0
O(11)···H(1BB)-N(1B)	153.6	O(5)···H(3DB)-N(3D)	143.9
O(12)···H(5BB)-N(5B)	154.1	O(6)···H(2DB)-N(2D)	146.7

[a] There are two independent molecules in the unit cell.

■ REFERENCES

(s1) Y. Onishi, Y. Nishimoto, M. Yasuda, K. Baba, *Org. Lett.*, 2014, **16**, 1176-1179.

(s2) F. Xu, Q. Wu, X. Chen, X. Lin, Q. Wu, *Eur. J. Org. Chem.*, 2015, **2015**, 5393-5401.

(s3) K. Kaczorowska, Z. Kolarska, K. Mitka, P. Kowalski, *Tetrahedron*, 2005, **61**, 8315-8327.

(s4) Z. Wang, Y.-T. Cui, Z.-B. Xu, J. Qu, *J. Org. Chem.*, 2008, **73**, 2270-2274.

(s5) A. S. Henderson, J. F. Bower, M. C. Galan, *Org. Biomol. Chem.*, 2014, **12**, 9180-9183.

(s6) T. Ankner, G. Hilmersson, *Org. Lett.*, 2009, **11**, 503-506.

(s7) N. S. Tulsi, A. M. Downey, C. W. Cairo, *Bioorg. Med. Chem.*, 2010, **18**, 8679-8686.

(s8) H. Zong, H. Huang, J. Liu, G. Bian, L. Song, *J. Org. Chem.*, 2012, **77**, 4645-4652.

(s9) A. K. Jha, S. Kishor, N. Jain, *RSC Adv.*, 2015, **5**, 55218-55226.

(s10) Y. Mei, P. Dissanayake, M. J. Allen, *J. Am. Chem. Soc.*, 2010, **132**, 12871-12873

(s11) D. Chávez-Flores, J. M. Salvador, *Biotechnol. J.*, 2009, **4**, 1222-1224.

(s12) S. K. Ghosh, K. G. Lewis, A. Kumar, J. A. Gladysz, *Inorg. Chem.*, 2017, **56**, 2304-2320 (the gas circulating flask is depicted in the supporting information).

(s13) Washing with water did not lead to any enrichment. The diastereomers exhibit diagnostic **C**HPh ^{13}C NMR chemical shift trends as detailed in reference s12.

(s14) E. Zhou, J. Zhang, Y. Lu, C. Dong, *ARKIVOC*, 2014, **2014**, 351-364.

(s15) K. Tanaka, T. Iwashita, C. Sasaki, H. Takahashi, *Tetrahedron: Asymmetry*, 2014, **25**, 602-609.

(s16) F. Yuste, R. Sánchez-Obregón, E. Díaz, M. A. García-Carrillo, *Tetrahedron: Asymmetry*, 2014, **25**, 224-228.

(s17) C. Wolf, A. M. Cook, J. E. Dannatt, *Tetrahedron: Asymmetry*, 2014, **25**, 163-169.

(s18) P. Borowiecki, *Tetrahedron: Asymmetry*, 2015, **26**, 16-23.

(s19) N. Jain, R. B. Patel, A. V. Bedekar, *RSC Adv.*, 2015, **5**, 45943-45955.

(s20) J. Kannappan, N. Jain, A. V. Bedekar, *Tetrahedron: Asymmetry*, 2015, **26**, 1102-1107.

(s21) G. Du, Y. Li, S. Ma, R. Wang, B. Li, F. Guo, W. Zhu, Y. Li, *J. Nat. Prod.*, 2015, **78**, 2968-2974.

(s22) M. S. Silva, D. Pietrobom, *New J. Chem.*, 2015, **39**, 8240-8244.

(s23) I. Pal, S. R. Chaudhari, N. R. Suryaprakash, *Magn. Reson. Chem.*, 2015, **53**, 142-146.

(s24) T. Laaksonen, S. Heikkinen, K. Wähälä, *Molecules*, 2015, **20**, 20873-20886.

(s25) S. H. Jung, K. Y. Kim, A. Ahn, S. S. Lee, M. Y. Choi, J. Jaworski, J. H. Jung, *New J. Chem.*, **2016**, *40*, 7917-7922.

(s26) G. Li, J. Cao, W. Zong, X. Lei, R. Tan, *Org. Chem. Front.*, 2016, **3**, 96-102.

(s27) A. E. Dowey, C. M. Puentes, M. Carey-Hatch, K. L. Sandridge, N. B. Krishna, T. J. Wenzel, *Chirality*, 2016, **28**, 299-305.

(s28) M. Uzarewicz-Baig, R.Wilhelm, *Heteroat. Chem.*, 2016, **27**, 121-134.

(s29) E. Monteagudo, P. March, A. Álvarez-Larena, A. Virgili, *ChemistrySelect*, 2017, **2**, 7362-7367.

(s30) V. Schurig, *Tetrahedron Lett.*, 1976, **17**, 1269-1272.

(s31) D. Magiera, A. Szmigielska, K. M. Pietrusiewicz, H. Duddeck, *Chirality*, 2004, **16**, 57-64.

(s32) C. Naumann, P. W. Kuchel, *J. Phys. Chem. A*, 2008, **112**, 8659-8664.

(s33) C. Naumann, P. W. Kuchel, *Chem. Eur. J.*, 2009, **15**, 12189-12191.

(s34) P. W. Kuchel, C. Naumann, B. E. Chapman, D. Shishmarev, P. Håkansson, G. Bacskay, N. S. Hush, *J. Magn. Reson.*, 2014, **247**, 72-80.

(s35) P. Berdagué, J.-E. Herber-Pucheta, V. Jha, A. Panossian, F. R. Leroux, P. Lesot, *New J. Chem.*, 2015, **39**, 9504-9517.